Chapter 4: Sulfur isotopic fractionation in the gas-phase oxidation of sulfur dioxide initiated by hydroxyl radicals*

4.1 Introduction

The oxidation of SO_2 is known to be the major source of tropospheric sulfate. According to current estimates, the homogeneous oxidation pathway accounts for more than half the total SO_2 processing [*Pitari et al.*, 2002]. Heterogeneous oxidation of sulfur dioxide by aqueous hydrogen peroxide, for which the sulfur isotopic enrichment factor has been estimated at 1.02, accounts for the remainder. Recent studies have also suggested that tropospheric SO_2 may contribute substantially to stratospheric sulfate [*Chin and Davis*, 1995; *Kjellstrom*, 1998; *Pitari et al.*, 2002; *Weisenstein et al.*, 1997].

Similar to the case of most species in the troposphere and the lower stratosphere, the homogeneous oxidation of SO_2 in the troposphere and lower stratosphere is driven by the OH radical. The gas-phase oxidation of sulfur dioxide into sulfuric acid is considered to proceed via the following scheme [*Fulle et al.*, 1999; *Jayne et al.*, 1997; *Kolb et al.*, 1994; *Li and McKee*, 1997; *Majumdar et al.*, 2000; *Morokuma and Muguruma*, 1994; *Tanaka et al.*, 1994; *Wine et al.*, 1984]:

$$SO_2 + OH + M \leftrightarrow HOSO_2 + M \qquad (4.1, -4.1)$$

$$HOSO_2 + O_2 \rightarrow HO_2 + SO_3 \qquad (4.2)$$

$$SO_3 + 2\ H_2O \rightarrow H_2SO_4 \cdot H_2O \qquad (4.3)$$

in which reaction (4.1) is rate-limiting [*Gleason et al.*, 1987].

---

* Adapted in part from Leung, F.Y., A.J. Colussi, and M.R. Hoffmann, Sulfur isotopic fractionation in the gas-phase oxidation of sulfur dioxide initiated by hydroxyl radicals, *J. Phys. Chem. A*, *105*, 8073-8076, 2001.

Elementary considerations suggest that the association of OH-radicals with SO_2 should display a *normal kinetic sulfur isotope effect* [*van Hook*, 1970b], that is, that the product should be depleted in the heavy isotope.

The isotopic composition of sulfate aerosol formed by oxidation of SO_2 released from remote sources will therefore depend ultimately on the relative importance of reaction (4.1) vs. heterogeneous oxidation by H_2O_2 [*Eriksen*, 1972; *Hegg and Hobbs*, 1978; *Tanaka et al.*, 1994]:

$$SO_2 + H_2O \rightarrow H^+ + HSO_3^- \quad (4.4)$$

$$HSO_3^- + H_2O_2 \rightarrow SO_4^{2-} + H^+ + H_2O \quad (4.5)$$

As noted in Chapter 1, it is possible to determine the isotopic fractionation of equilibrium processes given the vibrational frequencies of the reactants and products and a chemical channel between them. An analogous method exists to determine the kinetic isotopic fractionation rates given information about the transition state. We evaluate kinetic sulfur isotope effects for reaction (3.1) under atmospheric conditions using unimolecular reaction theory in conjunction with the most recent ancillary information, and also show by means of a simple 1-D model that our result is compatible with measured isotopic compositions of volcanically derived stratospheric sulfate.

4.2 Calculation of kinetic sulfur isotope effects in reaction 1

Calculations are based on rate constants for the unimolecular decomposition of the hydroxysulfonyl radical $HOSO_2$, k_{-1}, obtained by application of RRKM theory [*Forst*, 1973; *Robinson and Holbrook*, 1972], in conjunction with the ratio of overall equilibrium constants $^{34}K_1/^{32}K_1$ [*van Hook*, 1970b; *Weston*, 2001]:

$$\alpha = \frac{^{34}k_{4.1}}{^{32}k_{4.1}} = \frac{^{34}k_{-4.1}}{^{32}k_{-4.1}}\left[\frac{^{34}K_{4.1}}{^{32}K_{4.1}}\right] \tag{4.6}$$

which can be estimated from the corresponding ratio of molecular partition functions [*Benson*, 1976]:

$$\frac{^{34}K_{4.1}}{^{32}K_{4.1}} = \left[\frac{M_{HO^{34}SO_2}M_{^{32}SO_2}I^{1/3}_{HO^{34}SO_2}I^{1/3}_{^{32}SO_2}}{M_{HO^{32}SO_2}M_{^{34}SO_2}I^{1/3}_{HO^{32}SO_2}I^{1/3}_{^{34}SO_2}}\right]^{3/2}\left[\frac{Q_{HO^{34}SO_2}Q_{^{32}SO_2}}{Q_{HO^{32}SO_2}Q_{^{34}SO_2}}\right] \tag{4.7}$$

In Eq. (3.7), the M's are the molecular masses, the I's the products of the principal moments of inertia, and the Q's the harmonic vibrational partition functions:

$$Q = \prod_{i=1}^{3N-6}\frac{\exp(1.444\overline{\nu}_i/2T)}{1-\exp(-1.444\overline{\nu}_i/T)} \tag{4.8}$$

where the $\overline{\nu}_i's$ are vibrational mode energies in cm^{-1}. The molecular geometry and vibrational frequencies of the SO_2 isotopologues are well established [*Allavena et al.*, 1969]. We adopted the recently calculated *ab initio* structures for $HOSO_2$ (^2A) radicals [*Majumdar et al.*, 2000], and the corresponding transition state $[HO\text{---}SO_2]^{\ddagger}$ [*Li and McKee*, 1997]. Five of the nine internal vibrations of $HOSO_2$ sulfur isotopomers were observed by Kuo et al. [*Kuo et al.*, 1991]. The remaining four, which include the torsion of the -OH group, a $\widehat{O=S=O}$ bend, and two $\widehat{O-S=O}$ rocks, were assigned on the basis of Nagase et al. calculations [*Nagase et al.*, 1988]. The frequencies of the three SO_3-deformation modes in $HO^{34}SO_2$, which are expected to be sensitive to isotopic substitution, were constrained by the Teller-Redlich product theorem [*Nagase et al.*, 1988; *Robinson and Holbrook*, 1972; *van Hook*, 1970a; *van Hook*, 1970b]:

$$\prod_{i}^{3N-6} \frac{\overline{\nu}_{i,HO^{34}SO_2}}{\overline{\nu}_{i,HO^{34}SO_2}} = \left(\frac{M_{HO^{34}SO_2} I^{1/3}_{HO^{34}SO_2}}{M_{HO^{32}SO_2} I^{1/3}_{HO^{32}SO_2}} \right)^{3/2} \prod_{j}^{N} \left(\frac{m_{j,HO^{32}SO_2}}{m_{j,HO^{34}SO_2}} \right)^{3/2} \tag{4.9}$$

The retrieved or estimated parameters used in the calculations are collated in Table 4.1.

Table 4.1: Molecular parameters used in the calculations

Species	Parameters
OH	$\Delta H_{f,298\,K}$ = 39.46 kJ mol^{-1}; $S°_{298\,K}$ (standard state: 1 atm ideal gas) = 183.81 J K^{-1} mol^{-1}
$^{32}SO_2$	$\Delta H_{f,298\,K}$ = -296.86 kJ mol^{-1}; $S°_{298\,K}$ = 248.37 J K^{-1} mol^{-1}; M = 64 amu; $I^{1/3}$ = 28.66 amu Å^2; $\overline{\nu_i}$'s /cm^{-1} = 518, 1151, 1362
$^{34}SO_2$	M = 66 amu; $I^{1/3}$ = 28.99 amu Å^2; $\overline{\nu_i}$'s /cm^{-1} = 513, 1145, 1345
$HO^{32}SO_2$	$\Delta H_{f,298\,K}$ = -389 kJ mol^{-1}; $S°_{298\,K}$ = 290.80 J K^{-1} mol^{-1}; M = 81 amu; $I^{1/3}$ = 71.14 amu Å^2; $\overline{\nu_i}$'s /cm^{-1} = 3540, 1309, 1296, 1097, 759, 252, 500, 400 (2)
$HO^{34}SO_2$	M = 83 amu; $I^{1/3}$ = 71.26 amu Å^2; $\overline{\nu_i}$'s /cm^{-1} = 3540, 1293, 1289, 1090, 752, 252, 497, 397 (2)
$[HO\cdots^{32}SO_2]^{‡}$	$I^{1/3}$ = 87.64 amu Å^2; $\overline{\nu_i}$'s /cm^{-1} = 3638, 1100, 900, 300, 200, 100 (2), 80
$[HO\cdots^{34}SO_2]^{‡}$	$I^{1/3}$ = 87.82 amu Å^2; $\overline{\nu_i}$'s /cm^{-1} = 3638, 1090, 892, 297, 198, 99 (2), 80

Numerical application of the Rice, Rampersger, Kassel and Marcus (RRKM) theory to reaction (-4.1) requires specifying the entropy of the transition state, i.e., its geometry and vibrational spectrum, the energy barrier $E°_{-4.1}$ at 0 K, and the average Lennard-Jones diameter (σ = 4.1 Å) and well depth (ε = 115 cm^{-1}) values for the reactant-bath gas (M = N_2) interaction [*Gilbert and Smith*, 1990]. The net entropy of the transition state, $S°^{‡}$, can be obtained form the overall entropy change: $\Delta S°_{-4.1}$ = 248.37 + 183.81 - 290.80 = 141.38 J K^{-1} mol^{-1} (standard state: 1 atm = 760 Torr = 1.011 × 10^5 Pa ideal gas at 300 K), and the experimental value of the high pressure A-factor for reaction (4.1) [*Benson*, 1976; *Fulle et al.*, 1999]: $A_{1p,\infty} = A_{1c,\infty}/(e\mathrm{R'T})$ = (1.2 × 10^{-11} cm^3 molec^{-1} s^{-1}) × (6

$\times 10^{20}$) / (2.7172 × 0.082 L atm K^{-1} mol^{-1} × 300 K) = 1.08×10^{8} atm^{-1} s^{-1}, via detailed balance [Benson, 1976]:

$$A_{-4.1,\infty} = A_{4.1p,\infty} \exp(\Delta S^{o}_{-4.1}/k_B) = 10^{15.43} s^{-1} = (e k_B T/h) \exp[(S^{o\blacklozenge} - S^{o}_{HOSO_2})/k_B] \qquad (4.10)$$

The molecular properties assigned to $[HO\cdots{}^{32}SO_2]^{\ddagger}$ (Table 4.1) verifiably meet this condition. The critical energy for the dissociation of $HO^{32}SO_2$, reaction (-4.1), is given by: $^{32}E^{o}_{-4.1} = \Delta H^{\circ}_{-4.1,\,300\,K} + \int_{300K}^{0K} \Delta C^{\circ}_{-4.1,p}\, dT + E^{o}4_{.1} = (131.6 - 8.1 + 3.0) = 126.50$ kJ mol^{-1}. The corresponding value for $HO^{34}SO_2$ dissociation follows from: $^{34}E^{o}_{-4.1} = {}^{32}E^{o}_{-4.1}$ + ZPE($[HO\cdots{}^{34}SO_2]^{\ddagger}$) - ZPE($HO^{34}SO_2$) - ZPE($[HO\cdots{}^{32}SO_2]^{\ddagger}$) + ZPE($HO^{32}SO_2$) = 126.62 kJ mol^{-1}. Master equation treatment of weak collisions in the fall-off region further requires the average downward energy transferred per collision as input, for which we adopt a value of $\langle \Delta E_{down} \rangle$ = 200 cm^{-1}, consistent with an experimental average collisional efficiency $\beta_c \sim 0.2$ for N_2 [*Fulle et al.*, 1999; *Wine et al.*, 1984].

The results of the calculations are shown in Figures. 4.1 and 4.2.

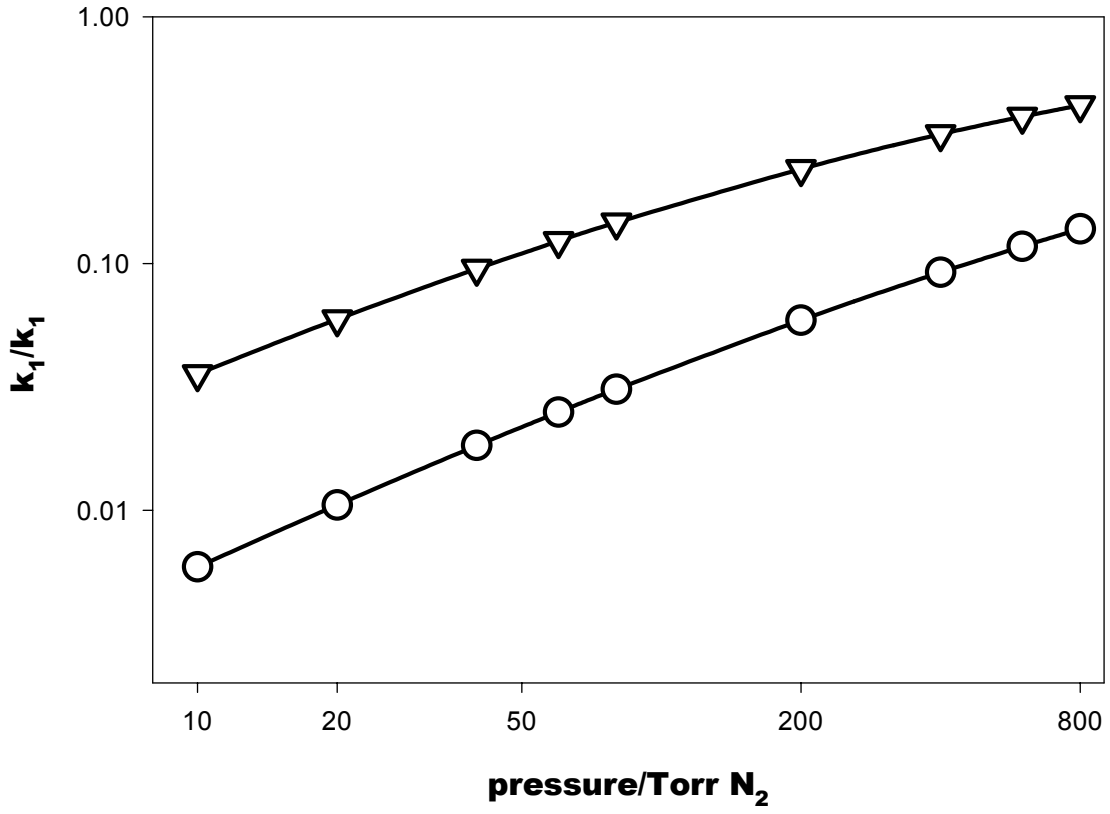

Figure 4.1: Fall-off curves $k_{-1}/k_{-1,\infty}$ for the unimolecular decomposition of $HO^{32}SO2$ in N_2. ○ : 200 K. triangle: 300 K.

Our calculated value of $^{32}k_{4.1} \sim 1 \times 10^{-13}$ cm^3 molecule^{-1} s^{-1} at [M] = 1×10^{18} molec cm^{-3}, 300 K, is within a factor of two of the experimental value, as measured by.*Wine et al.*, [1984], and *Fulle et al.*, [1999] in N_2 as a bath gas.

The most important result is that the sulfur isotopes actually induce an *inverse kinetic isotope effect*, i.e., $^{34}SO_2$ reacts faster than $^{32}SO_2$ in reaction (4.1). The unimolecular dissociation of the $HOSO_2$ radical, reaction (-4.1), behaves similarly. The reason for the latter is that the denser vibrational manifolds of both $HO^{34}SO_2$ and

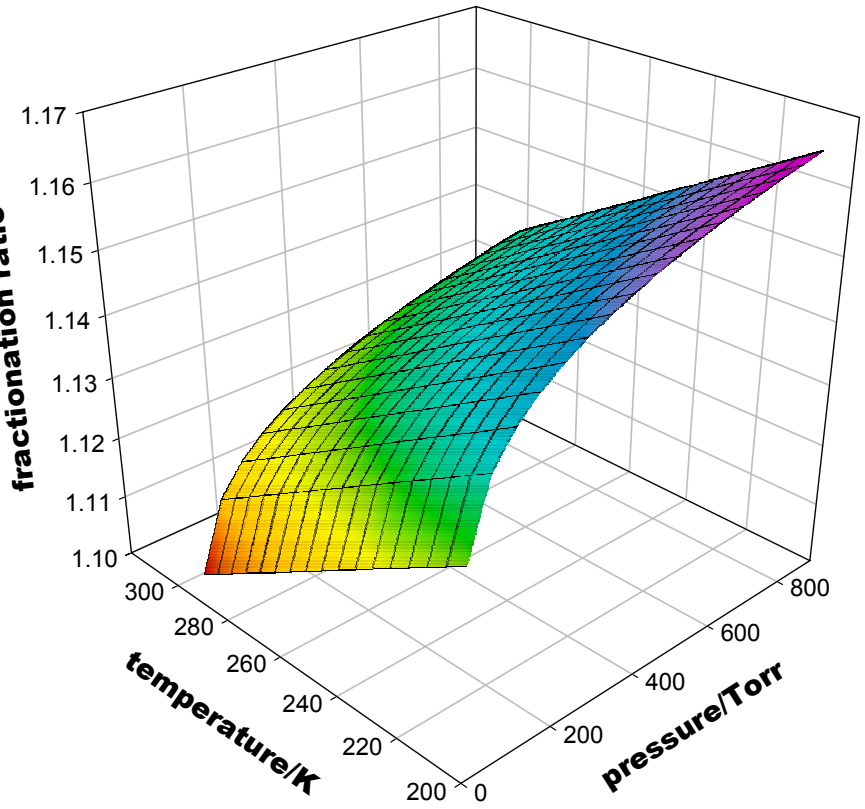

Figure 4.2: Fractionation ratios $\alpha = (k_{OH + {}^{34}SO_2})/(k_{OH + {}^{32}SO_2})$ as function of pressure and temperature. The depicted surface corresponds to:

$$\alpha = 1.1646 + 0.0198(P/Torr)^{0.1769} - 0.3092[(T/K)/1000]$$

$[HO\cdots{}^{34}SO_2]^{\ddagger}$ overcome the small, but positive difference of critical energies ${}^{34}E^{o}_{-4.1} - {}^{32}E^{o}_{-4.1} > 0$, that would otherwise cause a *normal isotope effect*, under all conditions. This outcome has a statistical origin. The ratio of the high pressure A-factors: ${}^{34}A_{-4.1,\infty}/{}^{32}A_{-4.1,\infty}$

= 1.096, accounts for a substantial fraction of the calculated effect. The ratio of equilibrium constants [($^{34}K_{4.1}/^{32}K_{4.1}$) = 1.048 and 1.031 at 200 K and 300 K, respectively, further adds to the trend (see Eq. 4.6).

The pressure and temperature dependences of the fractionation ratio α within the ranges covered in Fig. 4.2 (P/Torr ≤ 760 and 200 ≤ T/K ≤ 300) is given by Eq. 4.11.

$$\alpha = 1.1646 + 0.0198P^{0.1769} - 0.3092(T/1000) \qquad (4.11)$$

The parameters in Eq. 4.11 are most sensitive to the input $A_{1,\infty}$ value in Eq. 4.10, which, in conjunction with the estimated entropy of $HOSO_2$, determines $A_{-1,\infty}$ and the properties of the transition state as a consequence. As mentioned previously, we have adopted the most recent $A_{4.1,\infty} = 1.2 \times 10^{-11}$ molecule cm^{-3} s^{-1}, $E_{4.1}$ = 3.0 kJ mol^{-1} values derived by extrapolation of experimental rates determined up to 96 bar [*Fulle et al.*, 1999], instead of the lower values measured by Wine et al. below 1 bar [*Wine et al.*, 1984]. However, we notice that the derived $^{32}A_{4.1,\infty} = 10^{15.43}$ s^{-1} value (300 K) is consistent with a relatively loose transition state despite of the fact that reaction (1) involves the addition of OH-radicals to a closed-shell species [*Fulle et al.*, 1999; *Grela and Colussi*, 1987]. A lower $^{32}A_{4.1,\infty}$ value will result from a larger $S°_{HOSO_2}$ value but, again, we find no plausible arguments for making any such corrections, particularly vis-a-vis reliable, direct data [*Kuo et al.*, 1991; *Nagase et al.*, 1988]. Furthermore, a loose transition state would require a ratio $\rho = r^{\ddagger}_{S\text{-}OH}/r_{S\text{-}OH}$ somewhat larger than the ρ = 1.29 value based on *ab initio* calculated geometries [*Benson*, 1976; *Li and McKee*, 1997]. Bearing these uncertainties in mind, we performed a numerical sensitivity analysis indicating that a tenfold reduction in $A_{-4.1,\infty}$ will lower α by about 0.07 units across the (P, T) ranges investigated. In other words, any

adjustments to present parameters would not detract from our conclusion that $\alpha > 1.05$ under atmospheric conditions (Figure 4.3).

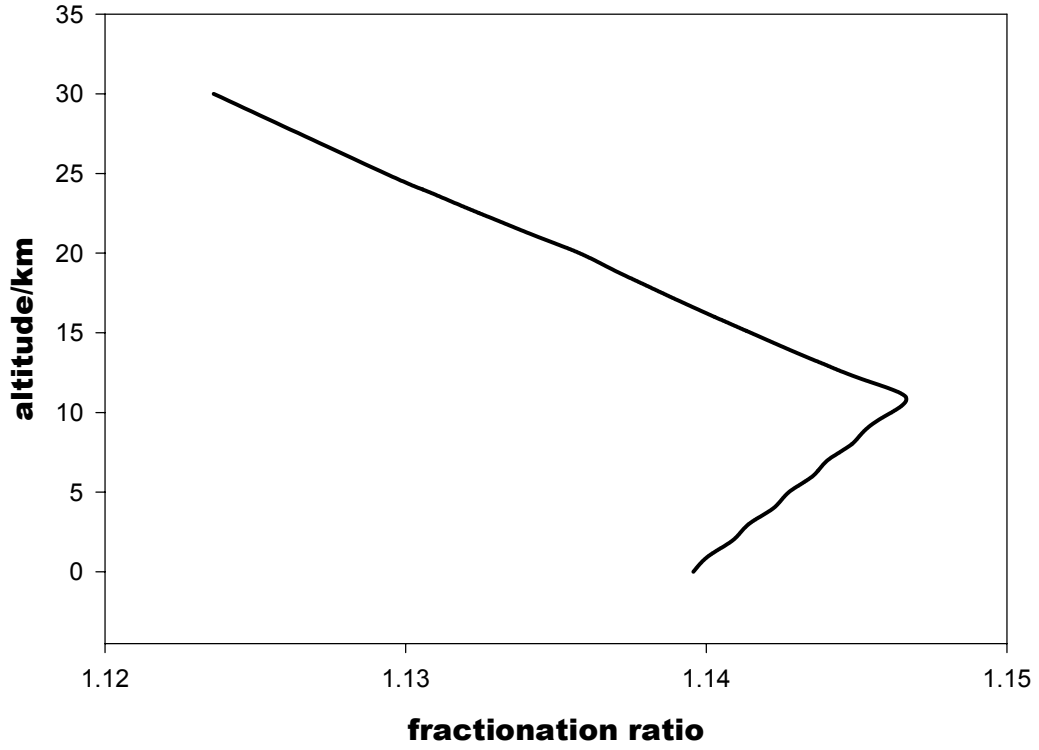

Figure 4.3: Fractionation ratios $\alpha = \alpha[P(z), T(z)]$ as function of the altitude z. The implicit $P(z)$ and $T(z)$ vertical profiles correspond to the 1976 standard atmosphere [*Seinfeld and Pandis*, 1998].

4.3 Discussion of results and 1-D modeling of evolution of sulfur isotopic composition of stratospheric sulfate following the 1963 eruption at Mt. Agung, Bali, Indonesia.

The above results help to interpret the early observations of Castleman et al. (1973) on the sulfur isotopic signatures of stratospheric sulfate aerosol following the major volcanic eruption of Mt. Agung [*Castleman et al.*, 1973; *Castleman et al.*, 1974]. Aerosol formed initially at 19 km altitude was enriched in ^{34}S, peaking at $\delta^{34}S \sim +20$ ‰

about 100 days after the eruption, an event that preceded maximum aerosol concentrations by about 200 days. The initial phase was followed by a precipitous decline of ^{34}S-sulfate aerosol abundance down to $\delta^{34}S = -24$ ‰ levels about 800 days after the eruption, before slowly recovering the background value of $\delta^{34}S = +2.6$ ‰ [*Castleman et al.*, 1974].

Given our present results of $\alpha > 1$, this behavior seems consistent with an OH-driven oxidation of a finite pool of stratospheric SO_2 into $^{34}SO_4$-enriched aerosol that subsequently undergoes removal by sedimentation. The ulterior fall-off of $\delta^{34}S$ values would naturally ensue from the progressive depletion of ^{34}S in the remaining SO_2 pool, a process known as Rayleigh distillation [*Griffith et al.*, 2000; *Newman et al.*, 1991], as shown by the solid lines in Figures 4.4a and b, which were generated by fitting the parameters of a conceptual 3-box, 1-D model to the available data, assuming that $\alpha > 1$ (See Appendix 4.1).

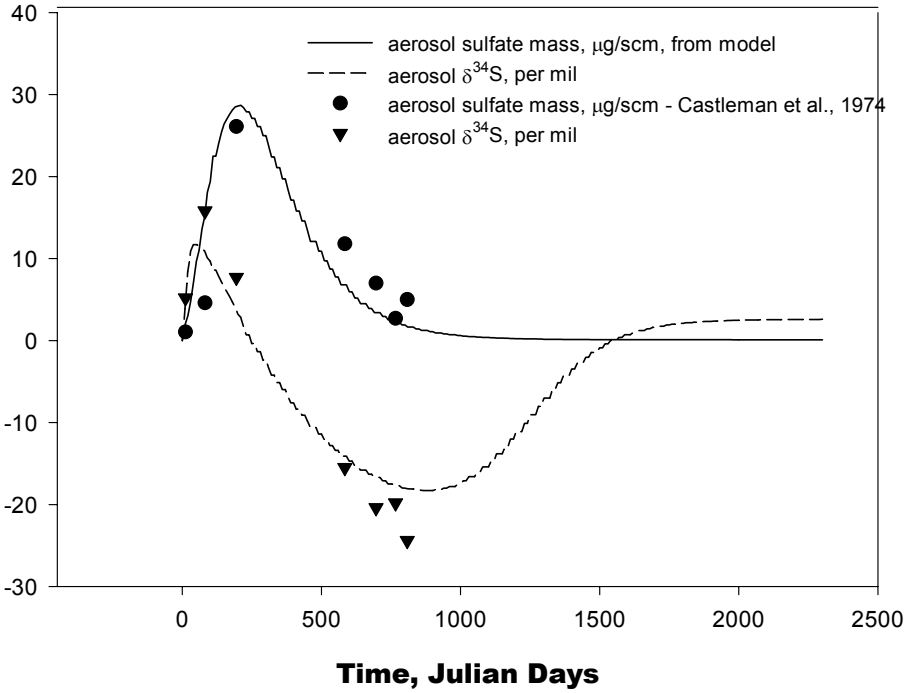

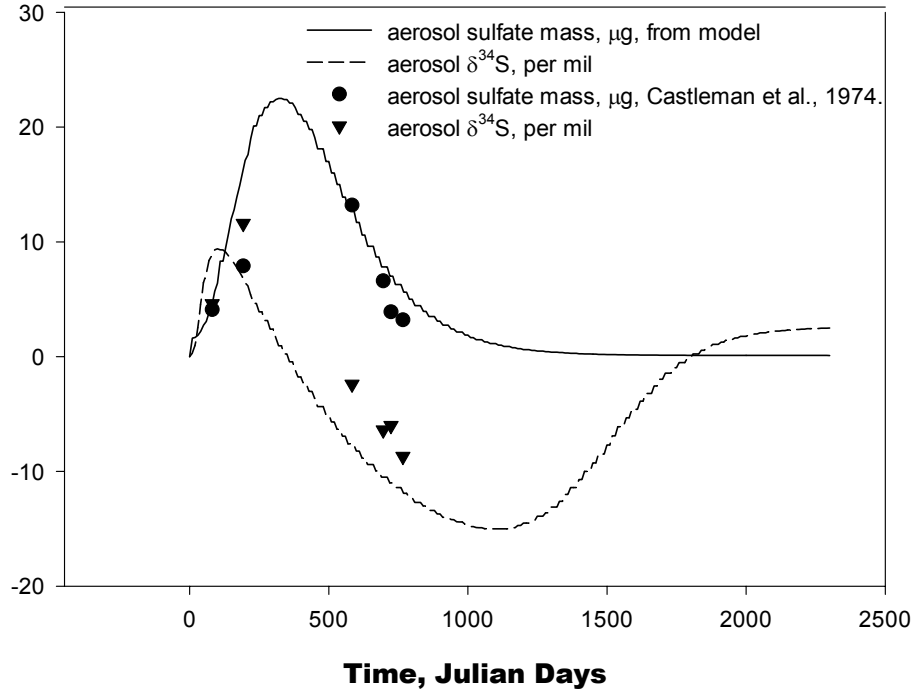

Figure 4.4: Comparison of model and measured results of stratospheric sulfate concentrations and $\delta^{34}S$ at a) ~5 °S and ~19 Km and b) 35 °S

The observed enrichment of tropospheric sulfate aerosol in ^{34}S relative to SO_2 [*Krouse and Grinenko*, 1991], together with the fact that SO_2 oxidation rates increase during the summer months [*Saltzman et al.*, 1983b], is also consistent with $\alpha > 1$ for the combined gas-phase oxidation processes, among which reaction (4.1) is the dominant reaction [*Eggleton and Cox*, 1978], despite suggestions to the contrary [*Saltzman et al.*, 1983a; *Tanaka et al.*, 1994].

References

Allavena, M., R. Rysnik, and D. White, Infrared spectra and geometry of SO_2 isotopes in solid krypton matrices, *J. Phys. Chem.*, *50*, 3399-, 1969.

Bekki, S., Oxidation of volcanic SO_2: a sink for stratospheric OH and H_2O, *Geophys. Res. Lett.*, *22*, 913-916, 1995.

Benson, S.W., *Thermochemical Kinetics*, Wiley Interscience, New York, 1976.

Castleman, J.A.W., H.R. Munkelwitz, and B. Manowitz, Contribution of volcanic sulphur compounds to the stratospheric aerosol layer, *Nature*, *244*, 345-346, 1973.

Castleman, J.A.W., H.R. Munkelwitz, and B. Manowitz, Isotopic studies of the sulfur component of the stratospheric aerosol layer, *Tellus*, *26*, 222-234, 1974.

Chin, M., and D.D. Davis, A reanalysis of carbonyl sulfide as a source of stratospheric background sulfur aerosol, *J. Geophys. Res.*, *100*, 8993-9005, 1995.

Eggleton, A.E.J., and R.A. Cox, *Atmos. Environ.*, *12*, 227, 1978.

Eriksen, T.D., Sulfur isotope effects, *Acta. Chim. Scan.*, *26*, 573-580, 1972.

Forst, W., *Theory of unimolecular reactions*, Academic Press, New York, 1973.

Fulle, D., H.F. Hamann, and H. Hippler, The pressure and temperature dependence of the recombination reaction HO + SO_2 + M => $HOSO_2$ + M, *Phys. Chem. Chem. Phys.*, *1*, 2695-2702, 1999.

Gilbert, R.G., and S.C. Smith, *Theory of Unimolecular and Recombination Reactions*, Blackwell Scientific Publications, Oxford (UK), 1990.

Gleason, J.F., A. Sinha, and C.J. Howard, Kinetics of the gas-phase reaction $HOSO_2+O_2$->HO_2+SO_3, *J. Phys. Chem.*, *91*, 719-724, 1987.

Grela, M.A., and A.J. Colussi, Systematic characterization of transition states for radical decompositions, *Int. J. Chem. Kinetics*, *19*, 869-879, 1987.

Griffith, D.W.T., G.C. Toon, B. Sen, J.F. Blavier, and R.A. Toth, Vertical profiles of nitrous oxide isotopomer fractionation measured in the stratosphere, *Geophys. Res. Lett.*, *27*, 2485-2488, 2000.

Hegg, D., and P. Hobbs, Oxidation of sulfur dioxide in aqueous systems with particular reference to atmosphere, *Atmos. Environ.*, *12*, 241-253, 1978.

Jayne, J., U. Poschl, Y. Chen, D. Dai, L. Molina, D. Worsnop, C. Kolb, and M. Molina, Pressure and temperature dependence of the gas-phase reaction of SO_3 with H_2O and the heterogeneous reaction of SO_3 with H_2O/H_2SO_4 surfaces, *J. Phys. Chem.*, *101*, 10000-10011, 1997.

Kjellstrom, E., A Three dimensional global model study of carbonyl sulfide in the troposphere and the lower stratosphere, *J. Atmos. Chem.*, *29*, 151-177, 1998.

Kolb, C., J. Jayne, D. Worsop, M. Molina, R. Meads, and A. Viggiano, Gas-Phase Reaction of sulfur-trioxide with water-vapor, *J. Am. Chem. Soc.*, *116*, 10314-10315, 1994.

Krouse, H.R., and V.A. Grinenko, editors, *Stable Isotopes: Natural and Anthropogenic sulphur in the Environment, Scope 43*, 400 pp., John Wiley and Sons, 1991.

Kuo, Y.-P., B.-M. Cheng, and Y.-P. Lee, Production and trapping of $HOSO_2$ from the gaseous reaction OH + SO_2: the infrared absorption of $HOSO_2$ in solid argon, *Chem. Phys. Lett.*, *177*, 195-199, 1991.

Li, W.-K., and M.L. McKee, Theoretical study of OH and H_2O addition to SO_2, *J. Phys. Chem.*, *101*, 9778-9782, 1997.

Majumdar, D., G.-S. Kim, J. Kim, K.S. Oh, and J.Y. Lee, Ab initio investigations on the $HOSO_2 + O_2$ => $SO_3 + HO_2$ reaction, *J. Chem. Phys.*, *112*, 723-730, 2000.

Morokuma, K., and C. Muguruma, Ab initio molecular-orbital study of the mechanism of the gas-phase reaction SO_3+H_2O - importance of the second water molecule, *J. Am. Chem. Soc.*, *116*, 10316, 1994.

Nagase, S., S. Hashimoto, and H. Akimoto, $HOSO_2$ and $HOSO_4$ Radicals studied by Ab initio Calculations and Matrix Isolation Technique, *J. Phys. Chem.*, *92*, 641-644, 1988.

Newman, L., H.R. Krouse, and V.A. Grinenko, Sulphur isotope variations in the atmosphere, in *Stable isotopes in the assessment of natural and anthropogenic sulphur in the environment*, edited by H.R. Krouse, and V.A. Grinenko, Wiley, New York, 1991.

Pitari, G., E. Mancini, V. Rizi, and D.T. Shindell, Impact of future climate and emission changes on stratospheric aerosols and ozone, *J. Atmos. Sci.*, *59*, 414-440, 2002.

Plumb, R.A., A "tropical pipe" model of stratospheric transport, *J. Geophys. Res.*, *101*, 3957-3972, 1996.

Rampino, M.R., and S. Self, Historic eruptions of Tambora (1815), Krakatau (1883) and Agung (1963), their stratospheric aerosols, and climatic impacts, *Quart. Res.*, *18*, 127-143, 1982.

Robinson, P.J., and K.A. Holbrook, *Unimolecular reactions*, chapter 9 pp., Wiley, London, 1972.

Saltzman, E.S., G.W. Brass, and D.A. Price, The mechanism of sulfate aerosol formation: chemical and sulfur isotopic evidence, *Geophys. Res. Lett.*, *10*, 513-516, 1983a.

Saltzman, E.S., G.W. Brass, and D.A. Price, The mechanism of sulfate aerosol formation: chemical and sulfur isotopic evidence, *Geophys. Res. Lett.*, *10*, 513, 1983b.

Seinfeld, J.H., and S.N. Pandis, *Atmospheric Chemistry and Physics: From Air Pollution to Climate Change*, 1326 pp., John Wiley and Sons, New York, New York, 1998.

Tanaka, N., D.M. Rye, Y. Xiao, and A.C. Lasaga, Use of stable sulfur isotope systematics for evaluating oxidation reaction pathways and in-cloud-scavenging of sulfur dioxide in the atmosphere, *Geophys. Res. Lett.*, *21*, 1519-1522, 1994.

van Hook, W.A., Isotope effects in chemical reactions, ACS Monograph 167, edited by C.J. Collins, and N.S. Bowman, pp. 1-84, New York, 1970a.

van Hook, W.A., Kinetic isotope effects: introduction and discussion of the theory, in *Isotope effects in chemical reactions*, edited by C.J. Collins, and N.S. Bowman, pp. 1-84, van Nostrand, New York, 1970b.

Weisenstein, D.K., G.K. Yue, M.K.W. Ko, N.-D. Sze, J.M. Rodriguez, and C.J. Scott, A two-dimensional model of sulfur species and aerosols, *J. Geophys. Res.*, *102*, 13019-13035, 1997.

Weston, J.R.E., Oxygen isotope effects in the oxidation of methane to carbon monoxide, *J. Phys. Chem. A*, 2001.

Wine, P.H., R.J. Thompson, A.R. Ravishankara, D.H. Semmes, T.A. Gump, and J.M. Nicovich, Kinetics of the reaction $OH+SO_2+M \rightarrow HOSO_2+M$ - temperature and pressure dependence in the falloff region, *J. Phys. Chem.*, *88*, 2095-2104, 1984.

Appendix 4.1 Conceptual model describing the evolution of SSA and the isotopic composition of SSA particles following the eruption at Mt. Agung, Bali, Indonesia in 1963.

A simple conceptual model (Figure 4.5) was constructed using a set of general parameters that are meant as proxies for the chemistry, microphysics and transport in the lower stratospheric system. The parameters were optimized using an optimizer facility in the FACSIMILE software to fit the data from March 1963 to May 18, 1965 in the southern hemisphere, where the bulk of the aerosol is located [*Rampino and Self*, 1982].

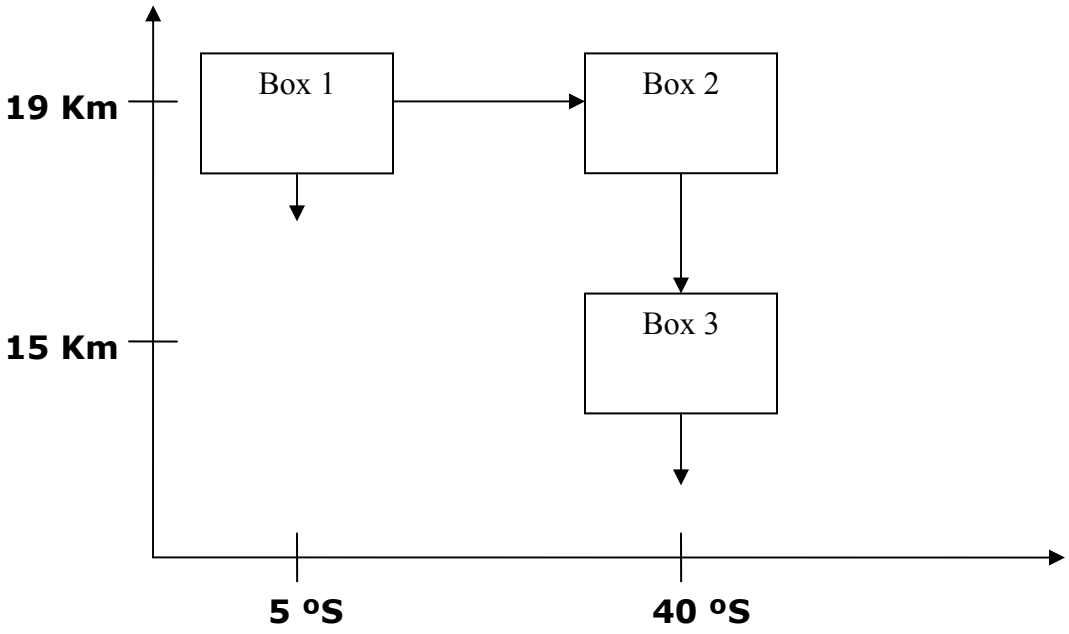

Figure 4.5: Schematic for Toy Model of evolution of volcanic aerosol following the 1963 Volcanic eruption at Mt. Agung, Bali, Indonesia.

Species are transported sequentially from Box 1 through Box 3 without mixing between the boxes. This roughly approximates the global diffuser model [*Plumb*, 1996].

The ^{34}S and ^{32}S isotopologues of $SO_{2(g)}$, $H_2SO_{4(g)}$, and $H_2SO_{4(aq)}$ were assumed to progress irreversibly in that order. The $H_2SO_{4(aq)}$ was separated into 3 size bins meant to represent aerosols of different sizes, and the relative removal rates of H_2SO_4 from each bin are scaled to the relative sedimentation velocities of particles of 0.1, 1, and 10 μm in diameter. Coagulation and condensation or evaporation are represented by equations that allow movement between the size bins.

An initial loading of 4500 μg-SO_4/scm of SO_2 is used. Given that the 1963 eruption ejected between 2.5 and 7 Tg of SO_2 [*Rampino and Self*, 1982], the initial loading into the stratosphere is equivalent to a volcanic plume distributed uniformly over a 0.4-1.2 cm wide band between 17-22 km altitude circumventing the equator. The adjustable parameters are optimized to fit the data using the FACSIMILE software.

However, the set of optimized parameters is not independent of the initial values. Although in our case, the optimized isotopic fractionation ratio (~1.02)was consistently about an order of magnitude lower than the fractionation ratio computed above, which suggests that heterogeneous chemistry may play an important role in processing of volcanic SO_2.

The conceptual model is able to reproduce the delay period after the eruption before the surge in the aerosol mass, which has also been observed by other researchers [*Bekki*, 1995], as well as the similar behavior in the sulfate $\delta^{34}S$, the maximum of which is offset from the maximum in the aerosol mass. The model also shows that a volcanic perturbation to the sulfur isotopic composition SSA is consistent with a Rayleigh distillation where $\varepsilon > 0$. However, given the overly simplistic nature of the conceptual

model, no firm conclusions regarding the magnitude of the isotopic enrichment factor of SO_2 oxidation can be inferred from the present calculations.